JACS
JOURNAL OF THE AMERICAN CHEMICAL SOCIETY

ARTICLE

pubs.acs.org/JACS

Transition-State Analysis of *Trypanosoma cruzi* Uridine Phosphorylase-Catalyzed Arsenolysis of Uridine

Rafael G. Silva, Mathew J. Vetticatt, Emilio F. Merino,[†] Maria B. Cassera,[†] and Vern L. Schramm*

Department of Biochemistry, Albert Einstein College of Medicine of Yeshiva University, 1300 Morris Park Avenue, Bronx, New York 10461, United States

Supporting Information

ABSTRACT: Uridine phosphorylase catalyzes the reversible phosphorolysis of uridine and 2′-deoxyuridine to generate uracil and (2-deoxy)ribose 1-phosphate, an important step in the pyrimidine salvage pathway. The coding sequence annotated as a putative nucleoside phosphorylase in the *Trypanosoma cruzi* genome was overexpressed in *Escherichia coli*, purified to homogeneity, and shown to be a homodimeric uridine phosphorylase, with similar specificity for uridine and 2′-deoxyuridine and undetectable activity toward thymidine and purine nucleosides. Competitive kinetic isotope effects (KIEs) were measured and corrected for a forward commitment factor using arsenate as the nucleophile. The intrinsic KIEs are: 1′-^{14}C = 1.103, 1,3-$^{15}N_2$ = 1.034, 3-^{15}N = 1.004, 1-^{15}N = 1.030, 1′-^{3}H = 1.132, 2′-^{2}H = 1.086, and 5′-$^{3}H_2$ = 1.041 for this reaction. Density functional theory was employed to quantitatively interpret the KIEs in terms of transition-state structure and geometry. Matching of experimental KIEs to proposed transition-state structures suggests an almost synchronous, S_N2-like transition-state model, in which the ribosyl moiety possesses significant bond order to both nucleophile and leaving groups. Natural bond orbital analysis allowed a comparison of the charge distribution pattern between the ground-state and the transition-state models.

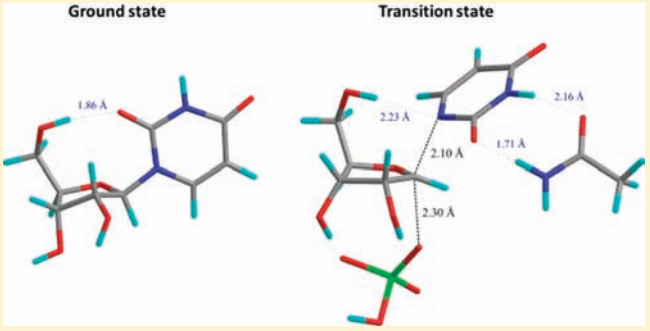

The kinetoplastid *Trypanosoma cruzi*, the etiologic agent of Chagas disease, possesses all genes codifying the six enzymes involved in de novo pyrimidine biosynthesis,[1] while the salvage pathway had only been suggested based on observation of uridine phosphorylase (UP) activity in cell extracts.[2] Recently, a putative nucleoside phosphorylase from the related protozoan *Trypanosoma brucei* was demonstrated to be a homodimeric UP, and a UP-specific region was identified and proposed to provide a tool to identify UPs from amino acid sequence alignments. The UP-specific region of the *T. brucei* genome was identified in *T. cruzi* and annotated as a putative nucleoside phosphorylase, which was then suggested to be a UP.[3]

Uridine phosphorylase (EC 2.4.2.3) catalyzes the reversible phosphorolysis of (2′-deoxy)uridine to form (2-deoxy)ribose 1-phosphate (R-1-P) and uracil[4] (Scheme 1A), an important step in the pyrimidine salvage pathway.[5] The reaction equilibrium favors nucleoside formation, and the equilibrium constant (K_{eq}) was calculated, using Haldane relationships, to be approximately 0.6.[6] This enzyme has been classified as a member of the nucleoside phosphorylase-I (NP-I) family, which includes enzymes that catalyze ribosyl transfer reactions, such as purine nucleoside phosphorylase (PNP) and methylthioadenosine phosphorylase (MTAP), on the basis of a common α/β-subunit fold and the inability to accept thymidine as substrate.[7]

Kinetic isotope effects (KIEs) have long been used to obtain information about reaction transition-state structure and geometry, since KIEs originate primarily from differences in bond vibration frequencies as a molecule goes from the ground state to the transition state in the course of a chemical reaction.[8,9] Transition-state analyses utilizing KIEs and computational modeling have been reported for both nonenzymatic and enzymatic ribosyl transfer reactions involving purine[10−12] and pyrimidine and pyridine[13−16] nucleosides and nucleotides. Some of these transition-state models served as blueprints for the design of transition-state analogues that act as potent enzyme inhibitors.[17,18]

Here the *T. cruzi* protein annotated as a putative nucleoside phosphorylase was expressed, purified to homogeneity, and demonstrated to be a uridine phosphorylase by substrate specificity studies. The oligomeric state of the protein was assessed by size-exclusion chromatography, and the substrate specificity was determined by steady-state kinetics. A combination of competitive KIEs measured with arsenate as nucleophile, isotope trapping experiment, and density functional theory (DFT) was employed to propose a transition-state model for the reaction catalyzed by *T. cruzi* UP (TcUP). The bond order and charge distribution differences between ground and transition states as well as the implications of the model for the chemical mechanism of the reaction are discussed.

Received: April 5, 2011
Published: May 20, 2011

Scheme 1. UP-Catalyzed (A) Phosphorolysis and (B) Arsenolysis of Uridine

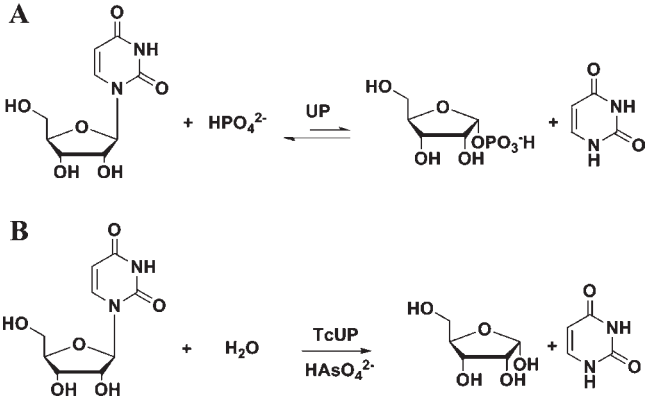

MATERIALS AND METHODS

Materials. D-[1-^{3}H]ribose, D-[1-^{14}C]ribose, and D-[6-$^3H_2$]glucose were purchased from American Radiolabeled Chemicals, Inc. D-[6-^{14}C]glucose was purchased from PerkinElmer, Inc. [1,3-$^{15}N_2$]Orotate and deuterium oxide were obtained from Cambridge Isotope Laboratories, Inc. Pyruvate kinase (PK), myokinase (MK), hexokinase (HK), glucose-6-phosphate dehydrogenase (G6PDH), glutamic acid dehydrogenase (GDH), 6-phosphogluconic acid dehydrogenase (6PGDH), and phosphoriboisomerase (PRI) were from Sigma-Aldrich. Alkaline phosphatase (AP) was from Roche. Ribokinase (RK) and phosphoribosyl-α-1-pyrophosphate synthetase (PRPPase) were prepared as previously described.[19,20] UMP synthase (UMPS) and [3-^{15}N]orotate were kind gifts from, respectively, Keith Hazleton and Yong Zhang of this laboratory. All other chemicals and reagents were obtained from commercial sources and were used without further purification.

Expression and Purification of TcUP. The expression vector pJexpress414 containing the DNA sequence annotated as a *T. cruzi* putative nucleoside phosphorylase (GeneDB ID Tc00.10470535095-69.100), with an N-terminal His tag-encoding sequence and optimized codons for heterologous expression in *Escherichia coli*, was obtained from DNA 2.0, Inc. The construct was transformed into *E. coli* BL21-(DE3) RIPL cells (Novagen). The transformed cells were grown in Luria−Bertani medium containing 100 μg mL^{-1} ampicillin, at 37 °C, to an $OD_{600\ nm}$ of 0.5 and induced by addition of isopropyl-1-thio-β-D-galactopyranoside to a final concentration of 1 mM. Cells were allowed to grow for an additional 15 h period and harvested by centrifugation at 20 800 g for 30 min. All purification procedures were carried out at 4 °C. Cells were resuspended and incubated for 30 min in 25 mL of buffer A (20 mM Tris−HCl, 5 mM imidazole, 500 mM NaCl, pH of 7.9) containing 0.2 mg mL^{-1} of lysozyme, 0.05 mg mL^{-1} of DNase I, and a tablet of complete protease inhibitor cocktail (Roche), disrupted with a French press and centrifuged at 48 000 g for 30 min to remove cell debris. The supernatant was loaded onto a Ni-NTA column pre-equilibrated with buffer A. The column was washed with 6 column volumes of buffer A and 10 column volumes of buffer B (20 mM of Tris−HCl, 50 mM of imidazole, 500 mM of NaCl, pH of 7.9). The adsorbed material was eluted with 6 column volumes of buffer C (20 mM of Tris−HCl, 150 Mm of imidazole, 500 mM of NaCl, pH of 7.9), analyzed by sodium dodecyl sulfate polyacrylamide gel electrophoresis (SDS-PAGE),[21] concentrated using a 10 000 Da molecular weight (MW) cutoff Amicon ultrafiltration membrane, dialyzed against 4 L of 100 mM HEPES pH of 7.5, and stored at −80 °C. Protein concentration was determined spectrophotometrically at 280 nm using the theoretical extinction coefficient (ε_{280}) of 19 410 M^{-1} cm^{-1} (http://expasy.org). The protein was further characterized by trypsin digestion and matrix-assisted laser desorption/ionization time-of-flight mass spectrometry (MALDI-TOF).

Oligomeric State Determination. The molecular mass of the purified protein was estimated by gel-filtration chromatography using a Sephacryl S-200 26/60 column (GE Healthcare). All samples were run at 0.5 mL min^{-1} in 100 mM of HEPES, pH of 7.5, at 4 °C. Bovine thyroglobulin (670 000 Da), bovine γ-globulin (158 000 Da), chicken ovalbumin (44 000 Da), horse myoglobin (17 000 Da), and vitamin B_{12} (1350 Da) (Bio-Rad) were employed as MW standards. The K_{av} value for each protein was calculated with eq 1, where V_e is the elution volume, V_t is the total column volume, and V_0 is the void volume. K_{av} was plotted against the logarithm of MW:

$$K_{av} = (V_e - V_0)/(V_t - V_0) \quad (1)$$

HPLC Method. The formation of pyrimidine or purine bases upon nucleoside phosphorolysis was assessed by reverse-phase chromatography, at room temperature, using an HPLC model 2487 (Waters) and an analytical C_{18} Delta Pak column (Waters) pre-equilibrated with 10 column volumes of 50 mM of triethylamine:acetic acid, pH of 5.0. Each sample was injected and run at 1.0 mL min^{-1} in the same buffer, and base and nucleoside elution were followed by the increase in absorbance at the appropriate wavelength. A typical reaction mixture (300 μL) contained 10 μM of TcUP, 100 mM of HEPES, pH of 7.5, 50 mM of phosphate, and 200 μM of nucleoside. Reactions were allowed to proceed for 45 min prior to HPLC analysis. Each nucleoside and the respective base were run as standards to determine their retention time. In control experiments, TcUP, nucleoside, and phosphate were omitted, one at a time, from the reaction mixture.

Enzymatic Assay and Substrate Specificity of TcUP. All assays were performed under initial rate conditions at 25 °C and 100 mM of HEPES, pH of 7.5, in 120 μL, unless otherwise stated. The decrease in absorbance at 282 nm upon conversion of (2′-deoxy)uridine to uracil ($\Delta\varepsilon$ = 1600 M^{-1} cm^{-1}),[22] in the presence of TcUP, in either phosphorolytic or arsenolytic (Scheme 1A or B, respectively) reactions, was monitored in an SX-20 stopped-flow spectrophotometer outfitted with a mercury−xenon lamp (Applied Photophysics). The substrate specificity and apparent steady-state parameters of the enzyme were determined by measuring TcUP activity in the presence of varying concentrations of one substrate and fixed, saturating concentrations of the other. In all cases, the concentration of TcUP was 20 nM. Each data point is the average of at least 10 replicates measured on the stopped-flow. The data were fitted to eq 2, where v is the initial rate, V is the maximal velocity, A is the concentration of the varying substrate, and K_M is the Michaelis constant for the varying substrate:

$$v = (VA)/(K_M + A) \quad (2)$$

Synthesis and Purification of Isotopically Labeled Uridines. [1′-^{3}H]UMP and [1′-^{14}C]UMP were enzymatically synthesized at 37 °C from [1-^{3}H]ribose and [1-^{14}C]ribose, respectively (Scheme S1 in the Supporting Information). Each reaction mixture contained 1 mM of ribose, 20 mM of phosphoenolpyruvate (PEP), 0.2 mM of ATP, 20 mM of $MgCl_2$, 1.2 mM of orotate, 100 mM of KH_2PO_4 (pH 7.5), 50 mM of KCl, 1 mM of DTT, 0.2 U mL^{-1} of PRPPase, 2 U mL^{-1} of PK, 2 U mL^{-1} of MK, 1 U mL^{-1} of UMPS, and 1 U mL^{-1} of RK.

For the synthesis of [5′-$^3H_2$]- and [5′-^{14}C]UMP, D-[6-$^3H_2$]- and D-[6-^{14}C]glucose were, respectively, utilized as precursors (Scheme S1 in the Supporting Information). Each reaction mixture contained 1 mM of glucose, 20 mM of PEP, 0.2 mM of ATP, 20 mM of $MgCl_2$, 1.2 mM of orotate, 140 mM of KH_2PO_4 (pH 7.5), 50 mM of KCl, 2.5 mM of DTT, 0.2 mM of $NADP^+$, 20 mM of α-ketoglutarate (α-KG), 5.5 mM of NH_4Cl, 0.2 U mL^{-1} of PRPPase, 2 U mL^{-1} of PK, 2 U mL^{-1} of MK, 1 U mL^{-1} of UMPS, 1 U mL^{-1} of G6PDH, 1 U mL^{-1} of 6PGDH,

0.5 U mL^{-1} of PRI, 1 U mL^{-1} of GDH, and 0.2 U mL^{-1} of HK. Orotate was replaced by [1,3-$^{15}N_2$]- and [3-^{15}N]orotate for the synthesis of [5′-^{14}C,1,3-$^{15}N_2$]- and [5′-^{14}C,3-^{15}N]orotate, respectively. To synthesize [5′-^{14}C,2′-^{2}H]UMP, the reaction mix with D-[6-^{14}C]glucose was prepared in D_2O. The deuterium was incorporated by the reaction catalyzed by PRI, and the deuterium content in the final product was determined by electrospray ionization mass spectrometry (ESI-MS).

Labeled UMPs, synthesized in 1 mL reaction volumes, were purified by HPLC using the same method described above. The solvent was evaporated by centrifugation under vacuum, and the pellet was dissolved in water. The labeled UMPs were converted to labeled uridines via the AP-catalyzed reaction, and the labeled uridines were purified with the same protocol utilized for UMP purification.

Determination of Forward Commitment Factor. The forward commitment (C_f) for uridine in the arsenolysis catalyzed by TcUP was measured by the isotope trapping method.[23] Pulse incubation mixtures (20 μL) containing 20 μM of TcUP, 50 μM of [5′-^{14}C]uridine, and 100 mM of HEPES, pH of 7.5, at 25 °C, were chased with a solution (480 μL) consisting of 2 mM of uridine, 100 mM of HEPES, pH of 7.5, and 1 mM of NaH_2AsO_4. After 5 s, the reactions were quenched with 50 μL of 1 N HCl and loaded onto charcoal columns (W. R. Grace & Co.) pre-equilibrated with 10 mM ribose in 10% ethanol (v/v). [5-^{14}C]Ribose was eluted with 3 mL of 10 mM ribose in 10% ethanol (v/v), dried by centrifugation under vacuum, and dissolved in 100 μL of water and 10 mL of scintillation fluid (PerkinElmer). Radioactivity was counted for 10 min in a Tricarb 2910 TR scintillation counter (PerkinElmer). The values obtained in the absence of arsenate were used as background to correct the others. The final value is the average of eight replicates in two independent experiments. C_f was calculated with eq 3, where C_f is the forward commitment, and Y is ratio of moles of ribose to moles of TcUP−uridine complex. The concentration of TcUP−uridine complex was calculated according to eq 4, where ES is the concentration of the TcUP−uridine complex, E is the total concentration of enzyme in the pulse, S is the total concentration of uridine in the pulse, and K_M is the Michaelis constant for uridine.

$$C_f = Y/(1-Y) \quad (3)$$

$$ES = (E \times S)/(S + K_M) \quad (4)$$

Measurement of KIEs. All KIEs were measured by the competitive radiolabel method,[20] at 25 °C. A typical reaction mixture (1 mL) contained 1 mM of NaH_2AsO_4, 10 nM of TcUP, 100 mM of HEPES, pH of 7.5, and 100 μM of uridine (^{3}H- and ^{14}C-labeled and cold carrier). The arsenolysis was allowed to proceed to 15−20% completion, then half of the reaction mixture was loaded onto charcoal columns (Grance). The remainder of the reaction was completely converted to products by addition of 4 μM of TcUP and loaded onto charcoal columns. Column pre-equilibration and elution steps as well as sample preparation for scintillation counting followed the same procedures described for the isotope trapping experiment. A sample with only [^{14}C]uridine was also counted as a standard. At least 10 replicates, in 2 independent experiments, were averaged for each KIE.

Samples were counted in dual-channel fashion, with the ^{3}H signal appearing only in channel 1 and the ^{14}C signal in both channels. The initial ratio of ^{3}H to ^{14}C counts per minute (cpm) was 2:1, and enough material was used so that at least 10 000 cpm of ^{14}C was obtained in channel 2. The total ^{3}H signal was assessed by eq 5, and the total ^{14}C signal by eq 6, in which ^{3}H is the total number of cpm for this isotope, ^{14}C is the total number of cpm for this isotope, channels 1 and 2 are the number of cpm in each channel, and r is the channel 1 to 2 ratio of ^{14}C standard.[20]

$$^3H = \text{channel } 1 - (\text{channel } 2 \times r) \quad (5)$$

$$^{14}C = \text{channel } 2 \times (1 + r) \quad (6)$$

Experimental KIEs were calculated and extrapolated to 0% reaction using eq 7, where R_f and R_0 are the ratios of heavy to light isotopes at partial and complete conversions, respectively, and f is the fraction of substrate conversion.

$$KIE = \ln(1-f)/\ln[1 - f \times (R_f/R_0)] \quad (7)$$

Computational Methods. The nucleophilic substitution reaction involving arsenate and uridine was studied by density functional theory (DFT) in B3LYP and using a 6-31G** basis set as implemented in Gaussian 09.[24] All ground-state structures were located as global minima, and frequency calculations performed on the optimized structures contained no imaginary frequencies. All located transition structures, with and without geometric constraints, possessed only one calculated imaginary frequency, a characteristic of first-order saddle points that correspond to true transition states.[25] The isotope effects for each of the theoretical transition structures were calculated from scaled theoretical vibrational frequencies using ISOEFF98.[26] Tunneling corrections were applied using a one-dimensional infinite parabolic barrier model.[27]

RESULTS AND DISCUSSION

Purification, Activity, And Oligomeric State of TcUP. The N-terminal His-tagged enzyme was successfully overexpressed and purified to homogeneity. MALDI-TOF-TOF mass spectrometry analysis confirmed that the amino acid sequence of the homogeneous protein was that annotated as a putative nucleoside phosphorylase from the *T. cruzi* genome.

In reaction mixtures containing either uridine or 2′-deoxyuridine and phosphate, uracil was formed (Figure 1). No nucleobase formation was detected when reaction mixtures contained thymidine, cytosine, orotidine, or any of the purine nucleosides. Controls without phosphate eliminated a hydrolytic reaction for uracil formation under conditions that would have detected a rate 10^{-6} that of phosphorolysis. Thus TcUP is a (2′-deoxy)uridine-specific uridine phosphorylase that does not catalyze nucleoside hydrolysis in the absence of phosphate, as do some purine and pyrimidine phosphorylases.[28,29] This is in agreement with the specificity proposed for most UP members of the NP-I family[7] but contrasts with the detected, though small, activity toward thymidine reported for *T. brucei* UP.[3] The lack of hydrolysis of uridine by TcUP may also relate to the chemical stability of its N-ribosidic bond, which is stable to 1 N of HCl at 100 °C for more than 3 days.[30]

Molecular sieve chromatography estimated the molecular weight of TcUP to be 76 000 ± 2280 Da. The calculated MW of the subunit, based on the amino acid sequence of the His-tagged protein, is 38 630 Da (http://expasy.org), suggesting that TcUP is a homodimer in solution. The same oligomeric state has been proposed for *T. brucei* UP.[3]

Substrate Specificity and Apparent Kinetic Parameters. The kinetic parameters for TcUP and uridine are in the range reported for *E. coli* UP[6] and human UP (Table 1).[31] The specificity of TcUP for uridine and 2′-deoxyuridine is comparable, evidenced by the similar values of the specificity constants (k_{cat}/K_M). Thus, the ribosyl 2′-OH group is not essential for substrate binding or catalysis. TcUP also accepts arsenate as nucleophile, as is observed for other nucleoside phosphorylases.[11,12,15]

Commitments to Catalysis. C_f, the forward commitment, is the probability of a substrate to proceed forward to catalysis, after the Michaelis complex is formed, as opposed to dissociating to free substrate. The reverse commitment (C_r) reflects the tendency

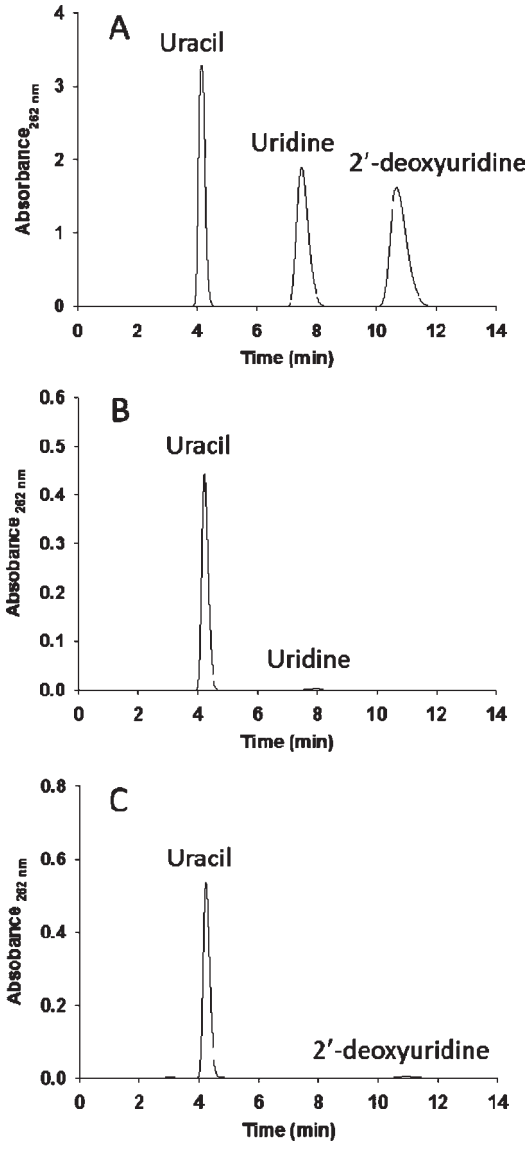

Figure 1. HPLC elution profile of TcUP-catalyzed reactions. (A) Uridine, 2′-deoxyuridine, and uracil run as standards. (B) Phosphorolysis of uridine. (C) Phosphorolysis of 2′-deoxyuridine.

Table 1. TcUP Apparent Steady-State Kinetic Parameters

varying substrate	k_{cat} (s^{-1})	K_M (μM)	k_{cat}/K_M (M^{-1} s^{-1})
uridine	12 ± 1	21 ± 2	5.7×10^5
phosphate		298 ± 23	4.0×10^4
2′-deoxyuridine	15 ± 1	32 ± 4	4.7×10^5
phosphate		385 ± 41	3.9×10^4
uridine	6 ± 1	20 ± 2	3.0×10^5
arsenate		183 ± 17	3.3×10^4

for the first enzyme−product complex following the isotope-sensitive step to undergo catalysis in the reverse direction instead of moving forward to free product and enzyme through the first irreversible step.[32] C_f always refers to the substrate carrying the isotopic label when dealing with competitive KIEs,[33] uridine in the present study. Significant commitment factors obscure KIE expression, and knowing their values permits calculation of intrinsic KIEs.[34] A C_f value of 0.283 ± 0.012 was measured for uridine with TcUP, using arsenate as a nucleophile. This value is similar to those reported for His257Phe (0.300 ± 0.010)[35] and Lys22Glu-His104Arg (0.239 ± 0.025)[36] mutants of human PNP and for Val39Thr-Asn123Lys-Arg210Gln mutant of bovine PNP (0.243 ± 0.026)[37] and permits correction of experimental KIEs to yield intrinsic values. The isotope trapping experiment establishes that uridine can bind to free enzyme, leading to a catalytically competent complex upon arsenate binding. The result eliminates a mandatory ordered kinetic mechanism in which the nucleophile binds to the free enzyme.

Experimental and Intrinsic KIEs. Competitive KIEs measured for the TcUP-catalyzed arsenolysis of uridine and their corresponding position and type are shown in Table 2. In enzymatic reactions, the competitive method provides isotope effects on V/K, therefore reporting on steps starting with free substrate up to and including the first irreversible step.[38] Quantitative information on the transition-state structure can only be gathered from intrinsic KIEs, the ones reporting on the microscopic chemical step of the enzymatic reaction.[33] Experimental KIEs can be corrected for C_f and C_r to yield intrinsic ones, according to eq 8, where ${}^{L}V/K$ is the experimental KIE on V/K, ${}^{L}k$ is the intrinsic KIE, and ${}^{L}K_{eq}$ is the isotope effect on the equilibrium constant.[39]

$$ {}^{L}V/K = ({}^{L}k + C_f + {}^{L}K_{eq} \times C_r)/(1 + C_f + C_r) \qquad (8) $$

Arsenate is used to replace phosphate in studies of nucleoside phosphorylase reactions inasmuch as the product ribose 1-arsenate is rapidly hydrolyzed to ribose. This renders the overall reaction irreversible and reduces eq 8 to 9, as C_r is negligible.[11] Accordingly, intrinsic KIEs for the TcUP-catalyzed reaction were obtained upon correction for C_f (Table 2). Further evidence that C_f is the only term reducing the experimental KIEs from their intrinsic values is provided by the 1-^{15}N KIE, which, after correction for C_f, is equal, within experimental error, to the maximum value found computationally for any possible mechanism or transition-state structure of this reaction (discussed below).[40]

$$ {}^{L}V/K = ({}^{L}k + C_f)/(1 + C_f) \qquad (9) $$

The large value of the 1′-^{14}C KIE and the relatively modest value of the 1′-^{3}H KIE suggest a bimolecular A_ND_N mechanism[41] with an S_N2-like transition state. In nucleophilic substitution reactions of nucleosides, large primary ^{14}C KIEs occur only with significant bond order between the developing oxocarbenium ion and both the leaving group and the attacking nucleophile at the transition state. The relatively small α-secondary ^{3}H KIE indicates incomplete sp^3 to sp^2 rehybridization at the transition state.[42] The large 1-^{15}N KIE is consistent with extensive, but not full, 1′-C to1-N bond loss at the transition state, with some bond order remaining,[43] as indicated by the 1′-^{14}C KIE. The large 2′-^{2}H KIE suggests significant hyperconjugation between the 2′-C−2′-H σ-bond and the developing vacant 1′-C p-orbital, forming a partial 1′-C−2′-C π-bond.[44] As the 2′-C−2′-H bond is weakened by electron density loss, the β-secondary ^{2}H KIE increases.[13] The isotope effects eliminate a steady-state ordered kinetic mechanism in which uridine is the first substrate to bind to the enzyme, as saturating arsenate concentration in this mechanism would decrease the KIEs to unity.[45] Interpretation of the intrinsic KIEs

dx.doi.org/10.1021/ja2031294 |J. Am. Chem. Soc. 2011, 133, 9923–9931

Table 2. Kinetic Isotope Effects for the TcUP-Catalyzed Arsenolysis of Uridine

heavy uridine	light uridine	type of KIE	experimental KIE	intrinsic KIE	predicted KIE
1′-^{3}H	5′-^{14}C[a]	α-secondary	1.103 ± 0.004	1.132 ± 0.005	1.126
1′-^{14}C	5′-$^{3}H_2$	primary	1.080 ± 0.003[b]	1.103 ± 0.004	1.109
5′-^{14}C,2′-^{2}H	5′-$^{3}H_2$	β-secondary	1.067 ± 0.003[b,c]	1.086 ± 0.004	1.080
5′-^{14}C,1,3-^{15}N	5′-$^{3}H_2$	primary and β-secondary	1.027 ± 0.003[b]	1.034 ± 0.004	1.027
5′-^{14}C,3-^{15}N	5′-$^{3}H_2$	β-secondary	1.003 ± 0.002[b]	1.004 ± 0.003	1.002
5′-^{14}C,1-^{15}N	–	primary	1.024 ± 0.004[d]	1.030 ± 0.005	1.025
5′-$^{3}H_2$	5′-^{14}C	δ-secondary	1.032 ± 0.002	1.041 ± 0.003	1.058

[a] The remote 5′-^{14}C KIE is assumed to be unity. [b] Experimental values corrected for remote 5′-$^{3}H_2$ KIE according to the equation KIE = $KIE_{obs} \times$ 5′-$^{3}H_2$ KIE. [c] Experimental values corrected for ^{2}H content according to the equation KIE = $(KIE_{obs} - 1 + F)/F$, where F is the fraction of ^{2}H in the substrate. [d] Experimental values corrected for 3-^{15}N KIE according to the equation KIE = KIE_{obs}/3-^{15}N KIE.

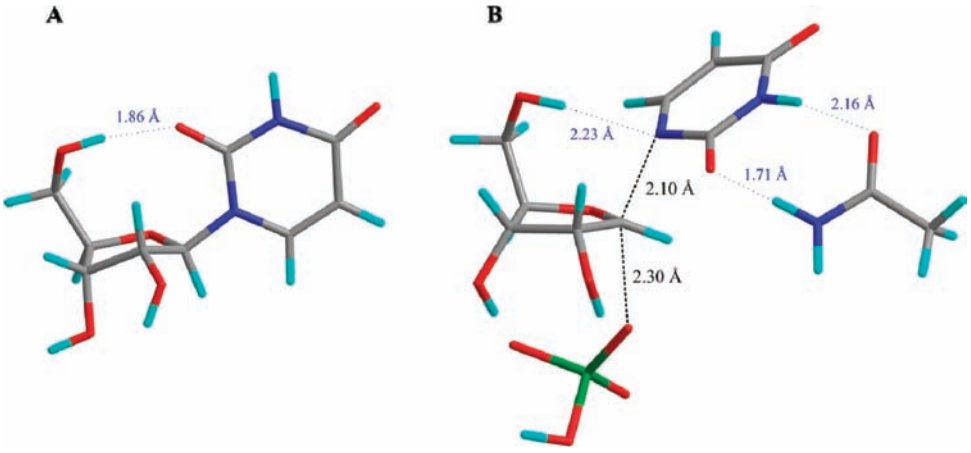

Figure 2. Stick models of DFT (B3LYP/6-31+G**)-optimized structures of (A) ground and (B) transition states. Carbon atoms are shown in gray, oxygen in red, hydrogen in cyan, nitrogen in blue, and arsenic in green. The dashed lines (black) represent r_{C-N} and r_{C-O}, and the dotted lines (blue) represent the distance between hydrogen and H-bond acceptor atoms. The full H-bond distances are described in the text.

in terms of transition-state structure was attempted using DFT-based modeling.

Ground-State and Transition-State Search. The lowest-energy reactant geometry was identified by optimizing uridine structures with distinct conformations of the ribosyl ring and orientations of uracil (coordinates for reactant structures are available in the Supporting Information). A structure with a 3′-exo ribosyl pucker and the 2-O of uracil poised to accept a hydrogen-bond (H-bond) from the 5′-OH was found to be the global minimum (Figure 2A). The choice of appropriate starting material is essential for accurate prediction of KIEs, as they reflect changes in bonding environment of atoms in the transition state relative to the lowest-energy initial material free in solution.[13]

A systematic search for transition structures was conducted by varying the distances between 1′-C and 1-N (r_{C-N}) and 1′-C and the nucleophilic oxygen of arsenate (r_{C-O}) (Scheme 2) by 0.2 Å increments. KIEs were calculated for every optimized structure and compared with intrinsic values (coordinates and predicted KIEs for all transition structure geometries are available in the Supporting Information). The geometry that best reproduced the intrinsic KIEs, particularly the distinct, large 1′-^{14}C KIE, was further analyzed, as the primary carbon KIE is the most informative one for investigation of transition-state structure and geometry of ribosyl-transfer reactions.[46]

Enzymatic Transition Structures and Predicted KIEs. The transition structures selected from the initial search were

Scheme 2. General Transition State for TcUP-Catalyzed Arsenolysis of Uridine

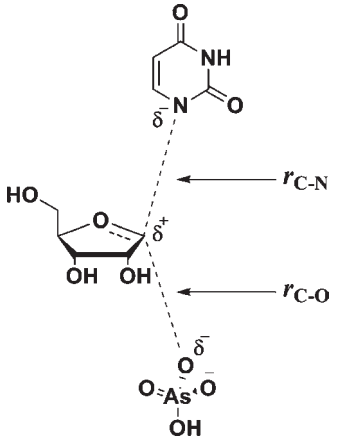

systematically modified in terms of r_{C-N} and r_{C-O}, with increments of 0.1 Å and of 5′-O−5′-C−4′-C−4′-O and of 2′-C−1′-C−1-N−2-C dihedral angles, and reoptimized. After calculation of KIEs for each structure, the best matches were selected upon comparison with intrinsic values (coordinates and predicted KIEs for transition structure geometries with varying dihedrals are available in the Supporting Information). An orientation with a

dx.doi.org/10.1021/ja2031294 |J. Am. Chem. Soc. 2011, 133, 9923–9931

H-bond between 5′-OH and 1-N yielded calculated KIEs in excellent agreement with intrinsic values and was stable enough to be maintained with different r_{C-N} and r_{C-O} even after the constraint on the 5′-O−5′-C−4′-C−4′-O dihedral angle was removed.

The orientation of uracil was important for accurate prediction of the 2′-^{2}H KIE. However, all transition structures that provided calculated KIE values in accordance with intrinsic ones were characterized by two imaginary frequencies, indicating that the structures were not located in first-order saddle points.[25] To overcome this difficulty, the side chain of an amino acid residue was added to the model. This approach has recently been successfully employed to model the transition states of the reactions catalyzed by human thymidine phosphorylase (TP)[15,29] and Phe200Gly mutant of human PNP.[47] As a three-dimensional structure of TcUP is not yet available, the crystal structure of *T. brucei* UP[3] was utilized to identify a residue that contacts uracil. The two enzymes share 100% amino acid sequence identity in the active site, and the chosen residue, glutamine (Gln) 248 (Gln249 in TcUP) is conserved in all uridine phosphorylases characterized.[3] The glutamine side chain was inserted in the transition-state model to stabilize the anionic uracil leaving group via H-bond contacts with the 2-O and 3-N of uracil anion, similarly to the crystal structure.[3] This orientation of uracil, with the 2-O directed away from the 5′-OH and 2′-H, provided a good match of the 2′-^{2}H KIE. The final transition structure (Figure 2B) possesses a 2′-C−1′-C−1-N−2-C dihedral angle of 85° and is characterized by a single imaginary frequency corresponding to motion along the reaction coordinate, and its calculated KIEs provide the best match for the intrinsic values (Table 2).

In the model represented in Figure 2B, r_{C-N} = 2.1 Å and r_{C-O} = 2.3 Å. Thus, TcUP-catalyzed arsenolysis of uridine proceeds via an almost synchronous A_ND_N transition state with moderate oxocarbenium ion character. This is in contrast with the dissociative transition-state models, with no significant participation of the attacking nucleophile, reported for inosine arsenolysis by bovine, malarial, and human PNP[11,46] and for the hydrolytic cleavage of the N-glycosidic bond of 2′-deoxyuridine in DNA, catalyzed by *E. coli* uracil DNA glycosylase (UDG),[48] while in agreement with the almost synchronous, though less tight, transition-state structure proposed for the NAD^+ hydrolysis catalyzed by diphtheria toxin.[43] S_N2 mechanisms have also been reported for *E. coli* UP phosphorolysis[49] and for human TP-catalyzed arsenolysis of thymidine, however in the latter, bond breaking was significantly more advanced than bond making at the transition state.[15]

A comparison of substrate and transition structures highlights the differences in forming the transition state. In reactant uridine, the 5′-OH group is oriented in a syn configuration, and the distance between the ribosyl 5′-O and the uracil 2-O is 2.82 Å, allowing an intramolecular H-bond (Figure 2A). At the transition state, the 5′-OH group is in a syn configuration but is positioned to form a H-bond with the leaving group 1-N, with a 5′-O−1-N distance of 3.18 Å, while the carbonyl 2-O is turned away from the ribosyl plane and interacts with the amino group of the glutamine side chain (Figure 2B). The ribosyl group of uridine has a 3′-exo and 2′-endo pucker (Figure 2A) and assumes a flatter conformation at the transition state, with a less pronounced 3′-exo pucker (Figure 2B). This conformation favors hyperconjugation between the 2′-C−2′-H bond and the partially unoccupied 1′-C p-orbital.[44] The syn configuration of the 5′-OH group and the distortion of the ribosyl pucker are features observed in other enzymatic N-ribosidic cleavage reactions and are proposed to be a strategy to help stabilize the charge development in the ribosyl moiety at the transition state.[11,43,48,50]

Table 3. Bond Distances and Pauling Bond Orders in the Ground-State and Transition-State Structures of TcUP-Catalyzed Reaction

bond	bond distance in ground state (Å)	bond distance in transition state (Å)	bond order in ground state[a]	bond order in transition state[a]
1′-C−1-N	1.47	2.10	1.00	0.35
1′-C−O(As)		2.30	–	0.25
1′-C−4′-O	1.41	1.31	1.07	1.49
1′-C−2′-C	1.55	1.53	0.98	1.03
1′-C−1′-H	1.09	1.04	1.00	1.18
2′-C−2′-H	1.09	1.10	1.00	0.98
4′-C−4′-O	1.45	1.48	0.97	0.92
5′-C−5′-O	1.41	1.42	1.07	1.03
4′-C−5′-C	1.53	1.52	1.03	1.07
1-N−2-C	1.40	1.37	1.27	1.40
1-N−6-C	1.38	1.36	1.35	1.44
3-N−2-C	1.38	1.39	1.35	1.31
3-N−4-C	1.41	1.41	1.22	1.22

[a] Bond orders >1 were calculated according to eq 10, while those <1 were calculated according to eq 11.

Pauling Bond Orders and Charge Distribution at the Transition State. Pauling bond order (n_{i-j}) is an exponential function of interatomic distance and represents the number of electron pairs shared by atoms i and j in a chemical bond.[51] Comparison of n_{i-j} values for bonds in the reactant state and the transition-state structures provides quantitative information on the geometry and hybridization of a molecule along the reaction coordinate. Accordingly, Pauling bond orders for specific bonds in uridine and in the transition structure were calculated using eq 10, for multiple bonds ($n_{i-j} > 1$), or eq 11, for partial bonds ($n_{i-j} < 1$), where n_{ij} is the bond order between atoms i and j, r_b is the bond length for a single bond between atoms of elements i and j, and r_{ij} is the bond length between atoms i and j.[52]

$$n_{ij} = e^{(r_b - r_{ij})/0.3} \quad (10)$$

$$n_{ij} = e^{(r_b - r_{ij})/0.6} \quad (11)$$

Bond orders (Table 3) are significant ($n_{C1'-N1}$ and $n_{C1'-O(As)}$ of 0.35 and 0.25, respectively) at the transition state, in agreement with the large intrinsic 1′-^{14}C and 1-^{15}N KIEs. Since n_{i-j} is a nonlinear function of bond distance, a small difference in length between bonds being broken and formed at the transition state (0.2 Å) reflects a significant difference in bond order. The gain in $n_{C1'-C2'}$ and the loss in $n_{C2'-H2'}$ as the reaction reaches the transition state agrees with hyperconjugation in the ribosyl moiety,[13] as discussed above, and explains the significant intrinsic 2′-^{2}H KIE. Incomplete sp^2 hybridization of 1′-C is indicated by the $n_{C1'-O4'}$ of 1.49, in conformity with the relatively modest intrinsic 1′-^{3}H KIE of 1.132. In comparison, $n_{C1'-O4'}$ = 1.65 at the transition state of human TP-catalyzed arsenolysis of thymidine, with 1′-^{3}H KIE = 1.177,[15] and $n_{C1'-O4'}$ = 1.71 at the transition state of inosine arsenolysis catalyzed by the Phe200Gly mutant of human PNP, for which 1′-^{3}H KIE = 1.254.[47] These

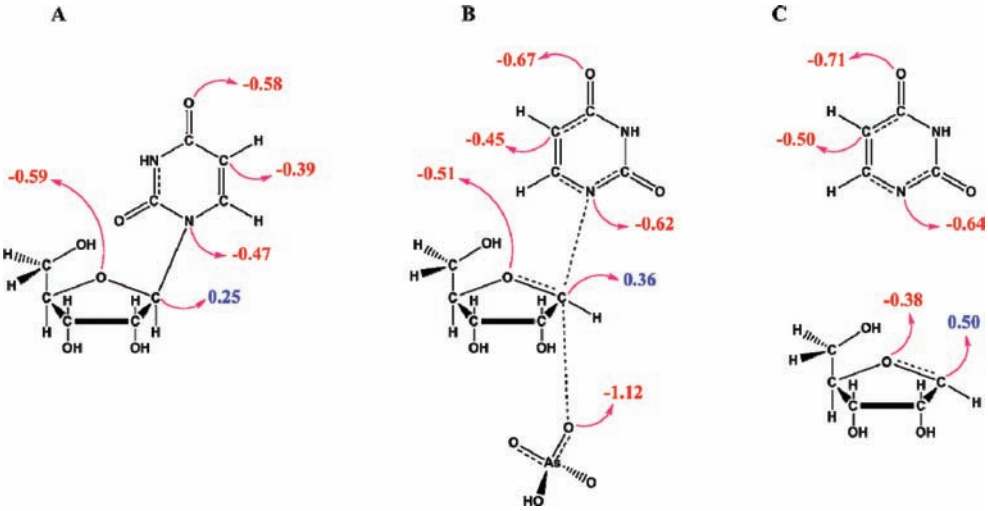

Figure 3. NBO charge distribution in (A) ground and (B) transition states of TcUP-catalyzed reaction and in (C) the theoretical intermediates in case the reaction proceeded by a stepwise mechanism. Negative charges are shown in red and positive charges in blue.

Scheme 3. Three General Nucleophilic Substitution Mechanisms Considered for TcUP-Catalyzed Arsenolysis of Uridine[a]

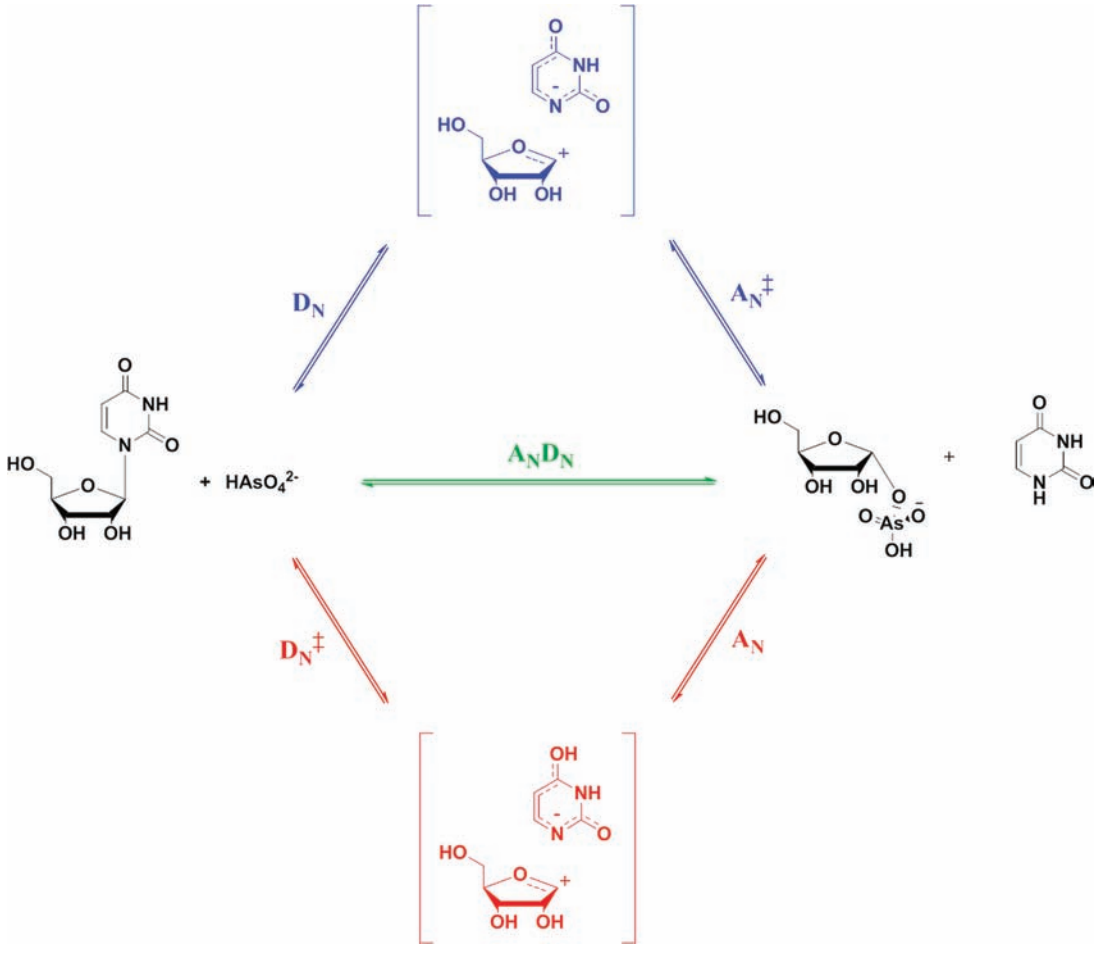

[a] In blue, $D_N{*}A_N^{\ddagger}$ stepwise mechanism; in green, A_ND_N concerted mechanism; in red, $D_N^{\ddagger}{*}A_N$ stepwise mechanism. The double dagger denotes the rate-limiting step.

two reactions proceed by highly asynchronous A_ND_N mechanisms, with more complete sp^2 character in the ribosyl moiety of their transition-state structures[15,47] than in the nearly synchronous A_ND_N mechanism reported here. A modest decrease in

dx.doi.org/10.1021/ja2031294 |*J. Am. Chem. Soc.* 2011, 133, 9923–9931

n_{N3-C2} is observed in the transition structure, consistent with the normal intrinsic 3-^{15}N KIE (Table 2). It is noteworthy that the bond order analysis of the DFT-derived transition-state model (Figure 2B) is in agreement with the qualitative interpretation of the intrinsic KIEs discussed above.

Atomic charge distribution of reactants and transition states is useful to understand catalytic strategies and transition-state analogue design.[53] Hence, natural bond orbital (NBO) charges were calculated for the TcUP transition-state model and compared with reactant uridine (Figure 3). As expected, the most conspicuous changes in NBO charges occur in the atoms along the reaction coordinate with 1′-C becoming more cationic and 1-N more anionic, as the N-ribosidic bonding electrons move toward uracil at the transition state. Concurrently, the attacking arsenate oxygen is partially bonded and therefore less negative at the transition state than in the reactant.[47] A small reduction in electron density occurs on 4′-O, since it forms a partial π-bond with 1′-C, as evidenced by the $n_{C1'-O4'}$ of 1.49. In the uracil moiety, 5-C and 4-O accumulate extra electron density in the transition structure, due to electron delocalization on the pyrimidine ring to stabilize the incoming N-ribosidic bond electrons. The negative charges on the uracil moiety at the transition structure may be slightly under-predicted in comparison with uridine, owing to the stabilization from a H-bond with the glutamine side chain. The glutamine amide donates a H-bond (2.74 Å) to the leaving group 2-O, while its carbonyl oxygen accepts a H-bond (3.15 Å) from the uracil 3-N (Figure 2B). Similar H-bond patterns are observed between Gln248 and product uracil in the *T. brucei* UP crystal structure.[3]

NBO charges were also calculated for the theoretical intermediates that would be formed if the reaction proceeded via a stepwise, S_N1 mechanism (Figure 3C). The most pronounced differences occur in the fully formed ribooxocarbenium ion, in which both 1-C and 4-O are significantly more deficient in electron density as compared with their counterparts in the S_N2-like transition state for TcUP-catalyzed reaction (Figure 3B). This attests to the relatively modest oxocarbenium ion character in the transition state for this reaction, as suggested above by the qualitative interpretation of the intrinsic KIEs.

Other Chemical Mechanisms. The intrinsic KIEs obtained here are consistent with a concerted, A_ND_N mechanism (Scheme 3, path in green). However, elimination of alternative mechanisms is also necessary. All bimolecular transition structures with a protonated leaving group failed to yield theoretical KIEs that matched the experimental values. Negatively charged nucleobases have also been described in the transition-state models of human and malarial orotate phosphoribosyl transferases,[14,54] human TP,[29] and uracil DNA glycosylase.[48]

In stepwise $D_N{}^*A_N{}^{\ddagger}$ mechanisms,[41,42] where the nucleobase departs first, followed by the rate-limiting attack of the nucleophile on the ribooxocarbenium ion (Scheme 3, path in blue), the KIEs are the product of the equilibrium isotope effect (EIE) for the first step and the KIE for the second step.[29,55,56] For uridine arsenolysis, the predicted 1,3-$^{15}N_2$ EIEs were in agreement with the intrinsic values for a negatively charged uracil (1.027) but did not match the calculated values for the departure of a neutral uracil with a proton on either 1-N (1.008) or 4-O (1.020) positions. In all cases, the products of the remaining EIEs and KIEs, for several r_{C-O}, were inconsistent with the experimental results, including that for the 1′-^{14}C KIE, where the largest predicted KIE for a $D_N{}^*A_N{}^{\ddagger}$ mechanism was 1.066.

A stepwise $D_N{}^{\ddagger}{}^*A_N$ mechanism,[41,42] involving the rate-determining break of the N-ribosidic bond and a subsequent nucleophilic attack on the ribooxocarbenium intermediate (Scheme 3, path in red), as described for bovine PNP-catalyzed arsenolysis of inosine,[11] was also considered. The largest calculated 1′-^{14}C KIE (1.070) for this mechanism was significantly smaller than the intrinsic value, ruling out this mechanism as a possibility. The last mechanism modeled was a $D_N{}^*A_N$ mechanism featuring an intermediate energetically similar to the transition state, with comparable barrier heights for bond breaking and formation, as proposed for the arsenolytic cleavage of inosine catalyzed by human PNP, in which all measured isotope effects were EIEs reporting on the formation of the ribooxocarbenium ion.[46] This mechanism is readily eliminated in the present work, since the predicted 1′-^{14}C EIE was essentially unity, the 1′-^{3}H EIE was three times as large as the intrinsic value, and the 5′-$^{3}H_2$ EIEs were inverse.

It should be pointed out that the term nucleophile-assisted S_N1 has been invoked to describe transition structures characterized by very low bond orders to both the leaving group and the latter, where the presence of the latter at the transition state is mandatory to yield calculated KIEs that match experimental values.[57] Nonetheless, the bond orders in the transition structure proposed for the TcUP reaction are significant, and reactions with transition structures of comparable bond order values to the ones presented here have widely been interpreted as S_N2.[15,42,55]

SUMMARY

The *T. cruzi* protein annotated as a putative nucleoside phosphorylase is a (2′-deoxy)uridine-specific homodimeric uridine phosphorylase that accepts arsenate as an alternative to phosphate as nucleophile. Intrinsic KIEs matched calculated KIEs for a DFT-derived transition-state model in which both the leaving group and the incoming nucleophile possess significant bond order to the electrophile being transferred, with r_{C-N} = 2.1 Å and r_{C-O} = 2.3 Å. The reaction proceeds via an A_ND_N chemical mechanism in which uracil departs as a negative species stabilized by interactions with the enzyme. The intrinsic KIEs are fully compatible with an A_ND_N mechanism and are inconsistent with other mechanisms for nucleophilic substitutions. Significant changes in Pauling bond orders and NBO charge distribution take place as the reaction proceeds from the ground to the transition state. To the best of our knowledge, this is the first report on the transition-state analysis of the reaction catalyzed by uridine phosphorylase from any organism.

ASSOCIATED CONTENT

Supporting Information. Synthetic scheme for labeled UMPs (Scheme S1) and geometries and calculated KIEs for transition structures. This material is available free of charge via the Internet at http://pubs.acs.org.

AUTHOR INFORMATION

Corresponding Author
vern@aecom.yu.edu

Present Addresses
[†]Department of Biochemistry, Virginia Polytechnic Institute and State University, Blacksburg, VA 24061, United States

■ ACKNOWLEDGMENT

This work was supported by NIH grant GM41916. The authors thank Yong Zhang and Keith Hazleton for their kind gifts of [3-^{15}N]orotate and UMP synthase, respectively, and Dr. Andrew S. Murkin and Dr. Luiz Pedro S. de Carvalho, respectively, for insightful discussion about reverse commitment and for critical reading of this manuscript.

■ REFERENCES

(1) Gao, G.; Nara, T.; Nakajima-Shimada, J.; Aoki, T. *J. Mol. Biol.* **1999**, *285*, 149–161.
(2) Miller, R. L.; Sabourin, C. L.; Krenitsky, T. A.; Berens, R. L.; Marr, J. J. *J. Biol. Chem.* **1984**, *259*, 5073–5077.
(3) Larson, E. T.; Mudeppa, D. G.; Gillespie, J. R.; Mueller, N.; Napuli, A. J.; Arif, J. A.; Ross, J.; Arakaki, T. L.; Lauricella, A.; Detitta, G.; Luft, J.; Zucker, F.; Verlinde, C. L.; Fan, E.; Van Voorhis, W. C.; Buckner, F. S.; Rathod, P. K.; Hol, W. G.; Merritt, E. A. *J. Mol. Biol.* **2010**, *396*, 1244–1259.
(4) Paege, L. M.; Schlenk, F. *Arch. Biochem. Biophys.* **1952**, *40*, 42–49.
(5) Pizzorno, G.; Cao, D.; Leffert, J. J.; Russell, R. L.; Zhang, D.; Handschumacher, R. E. *Biochim. Biophys. Acta* **2002**, *1587*, 133–144.
(6) Vita, A.; Huang, C. Y.; Magni, G. *Arch. Biochem. Biophys.* **1983**, *226*, 687–692.
(7) Pugmire, M. J.; Ealick, S. E. *Biochem. J.* **2002**, *361*, 1–25.
(8) Westheimer, F. H. *Chem Rev* **1961**, *61*, 265–273.
(9) Sims, L. B.; Fry, A.; Netherton, L. T.; Wilson, J. C.; Reppond, K. D.; Crook, S. W. *J. Am. Chem. Soc.* **1972**, *94*, 1364–1365.
(10) McCann, J. A.; Berti, P. J. *J. Am. Chem. Soc.* **2007**, *129*, 7055–7064.
(11) Kline, P. C.; Schramm, V. L. *Biochemistry* **1993**, *32*, 13212–13219.
(12) Singh, V.; Schramm, V. L. *J. Am. Chem. Soc.* **2006**, *128*, 14691–14696.
(13) Berti, P. J.; Schramm, V. L. *J. Am. Chem. Soc.* **1997**, *119*, 12069–12078.
(14) Zhang, Y.; Luo, M.; Schramm, V. L. *J. Am. Chem. Soc.* **2009**, *131*, 4685–4694.
(15) Schwartz, P. A.; Vetticatt, M. J.; Schramm, V. L. *Biochemistry* **2011**, *50*, 1412–1420.
(16) Cen, Y.; Sauve, A. A. *J. Am. Chem. Soc.* **2010**, *132*, 12286–12298.
(17) Miles, R. W.; Tyler, P. C.; Furneaux, R. H.; Bagdassarian, C. K.; Schramm, V. L. *Biochemistry* **1998**, *37*, 8615–8621.
(18) Singh, V.; Shi, W.; Evans, G. B.; Tyler, P. C.; Furneaux, R. H.; Almo, S. C.; Schramm, V. L. *Biochemistry* **2004**, *43*, 9–18.
(19) Singh, V.; Lee, J. E.; Nunez, S.; Howell, P. L.; Schramm, V. L. *Biochemistry* **2005**, *44*, 11647–11659.
(20) Parkin, D. W.; Leung, H. B.; Schramm, V. L. *J. Biol. Chem.* **1984**, *259*, 9411–9417.
(21) Laemmli, U. K. *Nature* **1970**, *227*, 680–685.
(22) Miller, R. L.; Lindstead, D. *Mol. Biochem. Parasitol.* **1983**, *7*, 41–51.
(23) Rose, I. A. *Methods Enzymol.* **1980**, *64*, 47–59.
(24) Frisch, M. J.; Trucks, G. W.; Schlegel, H. B.; Scuseria, G. E.; Robb, M. A.; Cheeseman, J. R.; Scalmani, G.; Barone, V.; Mennucci, B.; Petersson, G. A.; Nakatsuji, H.; Caricato, M.; Li, X.; Hratchian, H. P.; Izmaylov, A. F.; Bloino, J.; Zheng, G.; Sonnenberg, J. L.; Hada, M.; Ehara, M.; Toyota, K.; Fukuda, R.; Hasegawa, J.; Ishida, M.; Nakajima, T.; Honda, Y.; Kitao, O.; Nakai, H.; Vreven, T.; Montgomery, J. A., Jr.; Peralta, J. E.; Ogliaro, F.; Bearpark, M.; Heyd, J. J.; Brothers, E.; Kudin, K. N.; Staroverov, V. N.; Kobayashi, R.; Normand, J.; Raghavachari, K.; Rendell, A.; Burant, J. C.; Iyengar, S. S.; Tomasi, J.; Cossi, M.; Rega, N.; Millam, N. J.; Klene, M.; Knox, J. E.; Cross, J. B.; Bakken, V.; Adamo, C.; Jaramillo, J.; Gomperts, R.; Stratmann, R. E.; Yazyev, O.; Austin, A. J.; Cammi, R.; Pomelli, C.; Ochterski, J. W.; Martin, R. L.; Morokuma, K.; Zakrzewski, V. G.; Voth, G. A.; Salvador, P.; Dannenberg, J. J.; Dapprich, S.; Daniels, A. D.; Farkas, Ö.; Foresman, J. B.; Ortiz, J. V.; Cioslowski, J.; Fox, D. J. *Gaussian 09*, revision A.1; Gaussian, Inc.: Wallingford, CT, 2009.
(25) Hirschi, J. S.; Takeya, T.; Hang, C.; Singleton, D. A. *J. Am. Chem. Soc.* **2009**, *131*, 2397–2403.
(26) Anisimov, V.; Paneth, P. *J. Math. Chem.* **1999**, *26*, 75–86.
(27) Bell, R. P. *The tunnel effect in chemistry*; Chapman and Hall: London, 1980.
(28) Kline, P. C.; Schramm, V. L. *Biochemistry* **1992**, *31*, 5964–5973.
(29) Schwartz, P. A.; Vetticatt, M. J.; Schramm, V. L. *J. Am. Chem. Soc.* **2010**, *132*, 13425–13433.
(30) Prior, J. J.; Santi, D. V. *J. Biol. Chem.* **1984**, *259*, 2429–2434.
(31) Renck, D.; Ducati, R. G.; Palma, M. S.; Santos, D. S.; Basso, L. A. *Arch. Biochem. Biophys.* **2010**, *497*, 35–42.
(32) Northrop, D. B. *Annu. Rev. Biochem.* **1981**, *50*, 103–131.
(33) Cleland, W. W. *Methods Enzymol.* **1982**, *87*, 625–641.
(34) Schramm, V. L. *Methods Enzymol.* **1999**, *308*, 301–355.
(35) Murkin, A. S.; Birck, M. R.; Rinaldo-Matthis, A.; Shi, W.; Taylor, E. A.; Almo, S. C.; Schramm, V. L. *Biochemistry* **2007**, *46*, 5038–5049.
(36) Luo, M.; Li, L.; Schramm, V. L. *Biochemistry* **2008**, *47*, 2565–2576.
(37) Li, L.; Luo, M.; Ghanem, M.; Taylor, E. A.; Schramm, V. L. *Biochemistry* **2008**, *47*, 2577–2583.
(38) Cleland, W. W. *Arch. Biochem. Biophys.* **2005**, *433*, 2–12.
(39) Northrop, D. B. *Biochemistry* **1975**, *14*, 2644–2651.
(40) For this reaction, the computationally predicted $^{15}K_{eq} = 1.007$. Rearranging eq 7 to solve for ^{15}k, one obtains $^{15}k = {}^{15}(V/K) \times [1 + C_f] - C_f + [{}^{15}(V/K) - {}^{15}K_{eq}] \times C_r$, where the terms containing the corrections for C_f and C_r are explicitly separated. Substituting in the values found in this work, $^{15}k = 1.024 \times [1 + 0.283] - 0.283 + [1.024 - 1.007] \times C_r$, which is then further reduced to $^{15}k = 1.030 + 0.017 \times C_r$. Because the maximum calculated 1-^{15}N KIE on the arsenolysis of uridine equals ^{15}k, within experimental error, following correction for C_f, and C_r cannot assume negative values, it is clear that the only possible value for C_r is 0.
(41) Guthrie, R. D.; Jencks, W. P. *Acc. Chem. Res.* **1989**, *22*, 343–349.
(42) Berti, P. J.; McCann, J. A. *Chem Rev* **2006**, *106*, 506–555.
(43) Berti, P. J.; Blanke, S. R.; Schramm, V. L. *J. Am. Chem. Soc.* **1997**, *119*, 12079–12088.
(44) Hehre, W. J. *Acc. Chem. Res.* **1975**, *8*, 369–376.
(45) Cook, P. F.; Cleland, W. W. *Biochemistry* **1981**, *20*, 1790–1796.
(46) Lewandowicz, A.; Schramm, V. L. *Biochemistry* **2004**, *43*, 1458–1468.
(47) Silva, R. G.; Hirschi, J. S.; Ghanem, M.; Murkin, A. S.; Schramm, V. L. *Biochemistry* **2011**, *50*, 2701–2709.
(48) Werner, R. M.; Stivers, J. T. *Biochemistry* **2000**, *39*, 14054–14064.
(49) Komissarov, A. A.; Moltchan, O. K.; Romanova, D. V.; Debabov, V. G. *FEBS Lett.* **1994**, *355*, 192–194.
(50) Fedorov, A.; Shi, W.; Kicska, G.; Fedorov, E.; Tyler, P. C.; Furneaux, R. H.; Hanson, J. C.; Gainsford, G. J.; Larese, J. Z.; Schramm, V. L.; Almo, S. C. *Biochemistry* **2001**, *40*, 853–860.
(51) Pauling, L. *J. Am. Chem. Soc.* **1947**, *69*, 542–553.
(52) Houk, K. N.; Gustafson, S. M.; Black, K. A. *J. Am. Chem. Soc.* **1992**, *114*, 8565–8572.
(53) Schramm, V. L. *Annu. Rev. Biochem.* **1998**, *67*, 693–720.
(54) Zhang, Y.; Schramm, V. L. *J. Am. Chem. Soc.* **2010**, *132*, 8787–8794.
(55) Berti, P. J.; Tanaka, K. S. E. *Adv. Phys. Org. Chem.* **2002**, *37*, 239–314.
(56) Chen, X. Y.; Berti, P. J.; Schramm, V. L. *J. Am. Chem. Soc.* **2000**, *122*, 6527–6534.
(57) Gawlita, E.; Szylhabel-Godala, A.; Paneth, P. *J. Phys. Org. Chem.* **1996**, *9*, 41–49.